

Theoretically Feasible QoS in a MIMO Cellular Network Compared to the Practical LTE Performance

Mohamed Kadhem Karray
Orange Labs

38/40 rue Général Leclerc, 92794 Issy-Moulineaux France
E-mail: mohamed.karray@orange.com

Miodrag Jovanovic
Orange Labs

38/40 rue Général Leclerc, 92794 Issy-Moulineaux France
E-mail: miodrag.jovanovic@orange.com

Abstract—The objective is to build a global analytical approach for the evaluation of the quality of service perceived by the users in wireless cellular networks which is calibrated in some reference cases.

To do so, a model accounting for interference in a MIMO cellular system is firstly described. An explicit expression of users bit-rates theoretically feasible from the information theory point of view is then deduced. The comparison between these bit-rates and practical LTE performance permits to obtain the progress margins for potential evolution of the technology. Moreover, it leads to an analytical approximate expression of the system performance which is calibrated with the practical one. This expression is the keystone of a global analytical approach for the evaluation of the QoS perceived by the users in the long run of users arrivals and departures in the network. We illustrate our approach by calculating the users QoS as function of the cell radius in different mobility and interference cancellation scenarios.

Keywords—MIMO; interference; QoS; cellular; wireless

I. INTRODUCTION

The performance of a MIMO (*multiple input and multiple output*) cellular network may be considered from different points of view. The information theory gives the ultimate performance of the best possible coding schemes, whereas real systems deploy practical coding schemes of lower performance. On the other hand, information theory gives closed form formulae in several cases, whereas practical system performance is mostly evaluated by simulations such as those of 3GPP (*3rd Generation Partnership Project*) [1].

The objective of the present paper is to compare these two points of views in order to establish an analytical approximation of practical system performance. Our ultimate aim is to build a global analytical approach which is firstly calibrated using simulation results in some reference practical cases, and then used to study the relationships between the key network parameters and the QoS (*quality of service*) perceived by the users.

A. Related work

Telatar [2, Lemma 2] gives the capacity of a MIMO channel with fading and additive white Gaussian noise (without interference) from the information theory point of view. Different MIMO configurations are compared within this context by Foschini and Gans [3]. Blum et al. [4] study the capacity of a MIMO cellular network with flat Rayleigh fading. Tulino

and Verdu [5] apply random matrix theory to analyze this capacity. Tarok et al. [6] study the performance of space-time coding which generalizes the Alamouti's codes [7]. Diggavi and Cover [8] study the worst noise process for an additive channel under covariance constraints.

The 3GPP [1] evaluates the performance of LTE systems by simulations. Goldsmith and Chua [9] observed that practical coding schemes performance may be evaluated by a modification of the famous $\log_2(1 + \text{SNR})$ Shannon's formula. Mogensen et al. [10] have observed that the LTE capacity in the AWGN context is well approximated by this formula with a multiplicative coefficient. These ideas will be extended in the present paper to MIMO cellular networks with fading.

B. Paper organization

In Section II an explicit expression of users bit-rates feasible from the information theory point of view is given. This expression is compared to practical system performance in Section III. The progress margins for potential evolution of the technology are also presented in this section. Finally, the *global analytical* approach is illustrated in Section IV by evaluating the quality of service perceived by the users in *real* cellular networks accounting for their arrivals and departures.

II. THEORETICALLY FEASIBLE BIT-RATES

The aim of the present section is to establish closed-form expressions of users bit-rates which are theoretically feasible in MIMO cellular networks.

A. Model

Consider a wireless network composed of some disjoint geographic zones, called *cells*, each one being served by a single *base station* (BS) with MIMO antennas. The power transmitted by each BS is limited to some given maximal value. The network operates *Orthogonal Frequency-Division Multiple Access* (OFDMA) which we describe now. The frequency spectrum (allocated to the considered network) is divided into a given number of sub-carriers, which are made available to all base stations. Each BS allocates disjoint subsets of these sub-carriers to its users. Thus, any given user receives only other-BS *interference*; that is the sum of powers emitted by other BS on the sub-carriers allocated to him by his serving BS.

Assume that the bandwidth of each sub-carrier is smaller than the *coherence frequency* of the channel, so that we can consider that the *fading* in each sub-carrier is *flat*. That is, the output of the channel at a given time depends on the input only at the same instant of time. No assumption is made on the *correlation* of the fading processes of the different subcarriers (for a given user and a given BS). However, the fading processes for different users or base stations are assumed independent.

Time is divided into time-slots of length smaller than the *coherence time* of the channel, so that, for a given sub-carrier, the fading remains *constant during each time-slot* and the fading process in different time-slots may be assumed *ergodic*. (Such model for fading generalizes the so-called *quasi-static* model where the fading process at different time-slots is assumed to be independent and identically distributed.)

The codeword duration equals the time-slot, which is assumed sufficiently large so that the *capacity* within each time-slot may be defined in the *asymptotic* sense of information theory. Users perform *single user detection*; thus the interference is added to the *additive white Gaussian noise* (AWGN). The statistical properties of the interference are not known a priori since they depend of the codings of the other users. However the signals transmitted by different base stations are assumed independent.

B. Notations

The *covariance matrix* of a random column vector $X = (X_1, \dots, X_t)^T$ in \mathbb{C}^t is denoted by $\Gamma_X = E[XX^*]$ where X^* is the transpose complex conjugate of X . Observe for future reference that

$$X^*X = \sum_{j=1}^t |X_j|^2 \quad (1)$$

A random vector (X_1, \dots, X_t) in \mathbb{C}^t is called *circularly symmetric Gaussian* iff it is Gaussian and, each of its components X_i ($i \in [1, t]$) has i.i.d. centred real and imaginary parts.

Consider the downlink of a wireless cellular network. Let u be a base station serving some user through a MIMO channel with t transmitting and r receiving antennas having the following discrete-time model. At a given time instant n the channel output $Y_n \in \mathbb{C}^r$ is related to the channel input $X_{u,n} \in \mathbb{C}^t$ by the following relation

$$Y_n = H_u X_{u,n} + J_n + Z_n, \quad n = 1, 2, \dots \quad (2)$$

where $H_u \in \mathbb{C}^{r \times t}$ is the fading between the considered user and his serving base station u (fading is assumed constant over time for the moment), $J_n \in \mathbb{C}^r$ is the interference and the random noises Z_1, Z_2, \dots are i.i.d. with values in \mathbb{C}^r such that each Z_n is circularly-symmetric Gaussian with covariance matrix $\Gamma_{Z_n} = NI_r$ where N is a given positive constant and I_r is the identity matrix of dimension r . The channel input is subject to a power constraint of the form

$$\frac{1}{n} \sum_{k=1}^n X_{u,k}^* X_{u,k} \leq P, \quad n = 1, 2, \dots$$

where P is a given positive constant. Using Equation (1) we see that the above constraint concerns the power aggregated over all the t transmitters.

For each interfering base station $v \neq u$, let $X_{v,n}$ be its transmitted signal and H_v be the fading between the considered user and the base station v (recall that fading is assumed constant over time). Then the interference equals

$$J_n = \sum_{v \neq u} H_v X_{v,n} \quad (3)$$

C. Deterministic fading: Feasible rates

Assume in the present section that the fading is deterministic; i.e. not random.

The *capacity region* of the different users from the information theory point of view (optimized simultaneously over the transmitted signals of all the users) is still unknown. Nevertheless we will show that there is a particular point within this capacity region (i.e. a *feasible* set of users bit-rates) which is easy to establish and express. This point corresponds to the following assumptions:

- (A1) The signals transmitted by different base stations are independent.
- (A2) The signal $X_{u,n}$ transmitted by the serving base station is circularly-symmetric Gaussian with covariance matrix $\Gamma_{X_{u,n}} = \frac{P}{t} I_t$ (power equi-partition between the transmitting antennas).
- (A3) The signal $X_{v,n}$ transmitted by each interfering base station $v \neq u$ is circularly-symmetric Gaussian with a covariance matrix $\Gamma_v = \frac{P}{t} I_t$ (again power equi-partition between the transmitting antennas).
- (A4) The transmitted signals are independent from noises.
- (A5) The signals transmitted at different time instants are independent.

The covariance matrix of the interference (3) equals

$$\begin{aligned} \Gamma_J &= E[J_n J_n^*] \\ &= E \left[\sum_{v \neq u} H_v X_{v,n} \sum_{v' \neq u} X_{v',n}^* H_{v'}^* \right] \\ &= \sum_{v \neq u} H_v \Gamma_{X_{v,n}} H_v^* \\ &= \sum_{v \neq u} H_v \Gamma_v H_v^* = \frac{P}{t} \sum_{v \neq u} H_v H_v^* \end{aligned}$$

where the third equality is due to (A1) and for the fourth one is due to (A3). By (A4), the interference plus noise $Z'_n := J_n + Z_n$ is circularly-symmetric Gaussian [2, Lemma 4] with covariance matrix

$$\mathcal{N} := E[Z'_n Z_n'^*] = NI_r + \frac{P}{t} \sum_{v \neq u} H_v H_v^* \quad (4)$$

Moreover, using (A1)-(A4) the received signal Y_n is circularly-symmetric Gaussian with covariance matrix

$$\Gamma_Y = E[(H_u X_{u,n} + Z'_n)(X_{u,n}^* H_u^* + Z_n'^*)] = \frac{P}{t} H_u H_u^* + \mathcal{N}$$

Assumption (A5) permits to restrict ourselves to the mutual information at a given time-instant; that is

$$\begin{aligned} I(X_{u,n}; Y_n) &= h(Y_n) - h(Y_n | X_{u,n}) \\ &= h(Y_n) - h(Z'_n) \\ &= \log_2 \det(\pi e \Gamma_Y) - \log_2 \det(\pi e \mathcal{N}) \\ &= \log_2 \det \left(I_r + \frac{P}{t} H_u H_u^* \mathcal{N}^{-1} \right) \end{aligned}$$

where for the first equality we use [11, Theorem 1.6.2], for the third one we use [2, Lemma 2] and where \mathcal{N} is given by (4). Recall that the capacity from the information theory point of view, denoted by C , is the supremum of the mutual information over all the distributions of the input signal. Thus

$$C \geq \log_2 \det \left(I_r + \frac{P}{t} H_u H_u^* \mathcal{N}^{-1} \right)$$

The right-hand side of the above equation¹ gives a *feasible* bit-rate for the considered user. Since our assumptions (A1)-(A5) are the same for all the users, we get similar expressions for the feasible bit-rates of the other users and this *collection of bit-rates* of the different users is *feasible*.

Till now we didn't account for the propagation-losses L_u and $\{L_v\}_{v \neq u}$ induced by the distance and shadowing between the considered user and the serving and interfering base stations respectively. In order to account for these losses, the above formula should be modified as follows

$$C \geq \log_2 \det \left(I_r + \frac{P}{t} \frac{H_u H_u^*}{L_u} \mathcal{N}^{-1} \right) \quad (5)$$

where the noise plus interference covariance matrix \mathcal{N} is now given by

$$\mathcal{N} = N I_r + \frac{P}{t} \sum_{v \neq u} \frac{H_v H_v^*}{L_v} \quad (6)$$

Remark 1: Continuous-time. Consider a continuous-time model of the channel. Let w be the bandwidth of the considered sub-carrier. The results in the discrete-time extend to the continuous-time case, but the capacity bounds, such as the right-hand side of (5), should be multiplied by the bandwidth w of the considered sub-carrier. In other words, the $\log_2(\cdot)$ should be replaced by $w \times \log_2(\cdot)$.

D. Ergodic capacity

Consider now a given sub-carrier and multiple time-slots. Recall that we assumed that the fading for different time-slots are independent and identically distributed. By the law of large numbers, the capacity averaged over a large number of time-slots would approach the so-called *ergodic capacity* $E[C]$ where the expectation is with respect to the fading states. No assumption is made on the distribution of the fading matrix H_v except that its covariance equals identity; that is

$$E[H_v H_v^*] = I_r, \quad \text{for all BS } v$$

which means that the fadings of two different transmitting antennas are decorrelated and that the fading second moment for a given antenna equals 1. The following proposition gives a lower bound for the ergodic capacity.

Proposition 1: The ergodic capacity of the channel (2) is lower bounded by

$$E[C] \geq E[\log_2 \det (I_r + \text{SINR} H_u H_u^*)] \quad (7)$$

where the expectation is with respect to the fading H_u with the serving BS and

$$\text{SINR} = \frac{(P/t)/L_u}{N + (P/t) \sum_{v \neq u} 1/L_v} \quad (8)$$

which may be viewed as the *Signal to Interference and Noise Ratio* per transmitting antenna².

¹which is coherent with [4, Equation (2)]

² See [5, Equation (3.169)].

Proof: Note that the expectations in the present proof are with respect to the fading random matrices with the serving BS H_u and with the interfering BS $\{H_v\}_{v \neq u}$. Let $E[\cdot|H_u]$ designates the expectation conditionally to H_u . By the properties of the conditional expectation, we have $E[C] = E[E[C|H_u]]$. Equation (5) implies that

$$E[C|H_u] \geq E \left[\log_2 \det \left(I_r + \frac{P}{t} \frac{H_u H_u^*}{L_u} \mathcal{N}^{-1} \right) \middle| H_u \right]$$

where \mathcal{N} is given by (6). Using the convexity of the function $\mathcal{N} \mapsto \log_2 \left[\det \left(I_r + \frac{P}{t} \frac{H_u H_u^*}{L_u} \mathcal{N}^{-1} \right) \right]$ on the set of positive definite matrices of $\mathbb{C}^{r \times r}$ (see [8, Lemma II.3]) and Jensen's inequality, we deduce that

$$\begin{aligned} E[C|H_u] &\geq \log_2 \det \left(I_r + \frac{P}{t} \frac{H_u H_u^*}{L_u} E[\mathcal{N}|H_u]^{-1} \right) \\ &= \log_2 \det \left(I_r + \frac{P}{t} \frac{H_u H_u^*}{L_u} E[\mathcal{N}]^{-1} \right) \\ &\geq \log_2 \det (I_r + H_u H_u^* \text{SINR}) \end{aligned}$$

where SINR is given by (8). Thus

$$E[C] = E[E[C|H_u]] \geq E[\log_2 (1 + H_u H_u^* \text{SINR})]$$

The right-hand side of (7) may be calculated by using [2, Theorem 2].

III. THEORETICAL VERSUS PRACTICAL PERFORMANCE

The objective of the present section is to compare the theoretical expression established in the previous section to practical LTE performance.

A. AWGN

Consider firstly a user served by a base station through an additive white Gaussian noise (AWGN) SISO channel without neither fading nor interference for the moment. The user gets ideally (i.e. in the asymptotic sense of information theory) a bit-rate given by the famous Shannon's formula $w \log_2 \left(1 + \frac{P/L_u}{N} \right)$ where w is the bandwidth allocated to the considered user, N is the noise power, P is the power transmitted by the BS and L_u is the propagation-loss (thus P/L_u is the received power). In order to get rid of the dependence of the bit-rate on the bandwidth, we define the *spectral efficiency* as the ratio of the bit-rate by the bandwidth which equals $\log_2 \left(1 + \frac{P/L_u}{N} \right)$ in the AWGN context.

Mogensen et al. [10] and the 3GPP [12, §A.2] have observed that the LTE system spectral efficiency in this AWGN context is well approximated by

$$s \simeq a \log_2 \left(1 + \frac{P/L_u}{N} \right) \quad (9)$$

for some constant $a < 1$ accounting on the one hand for the gap between the practical coding schemes and the optimal ones and on the other hand for the loss of capacity due to signalling. This observation shall be confirmed and the typical value of a for LTE will be given. Note that the relative difference $1 - a$ between the Shannon's limit and the practical LTE system may be seen as a progress margin for potential evolution of the technology in the AWGN context.

In the AWGN context, the 3GPP [12, §A.2] shows that there is a 25% gap between the practical coding schemes and

the optimal ones (in the sense information theory). Moreover, some of the transmitted bits are used for signalling which induces a supplementary capacity loss of about 30% (see [13, §6.8],[14, p.155]); this leads to $a = 0.75 \times (1 - 0.3) \simeq 0.5$ in Equation (9). Figure 1 shows that the spectral efficiency obtained by simulations with Orange's link tool agrees with the analytic approximation (9) with $a = 0.5$.

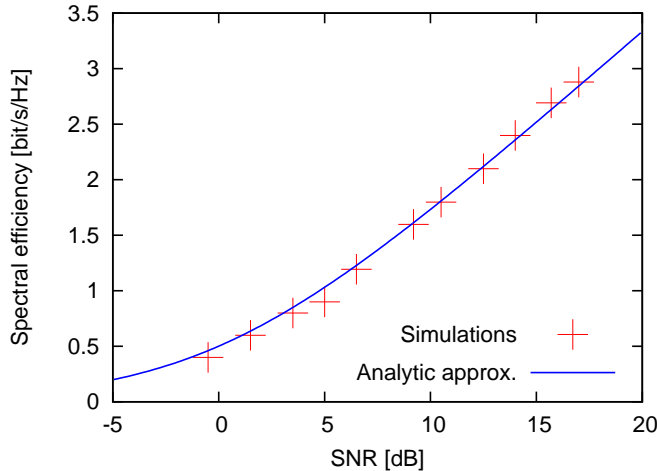


Fig. 1. Practical performance for AWGN

Remark 2: Indeed the signalling loss depends on the number of transmitting and receiving antennas. It is about $40/168 = 24\%$, $48/168 = 29\%$ and $52/168 = 31\%$ respectively for SIMO 1×2 , MIMO 2×2 and MIMO 4×2 (see [13, §6.8],[14, p.155]).

B. Fading and interference

We aim now to account for fading, MIMO and interference. In this context, let the *spectral efficiency* be the ratio of the bit-rate averaged over the fading (called ergodic capacity in the information theory framework) by the bandwidth.

In order to simplify the notation, we denote by S the analytical (lower bound of the) spectral efficiency given in the right-hand side of (7) pondered by the parameter $a = 0.5$ obtained in the previous section; that is

$$S(\text{SINR}, t, r) = aE[\log_2 \det(I_r + H_u H_u^* \text{SINR})] \quad (10)$$

where SINR is the signal to interference and noise ratio (per transmitting antenna) given by Equation (8).

The question now is what is the practical LTE spectral efficiency compared to the above analytical expression? Is it better or worse and what is the difference?

In order to get the practical LTE performance, we consider the output of Orange's simulator compliant with the 3GPP recommendation [1] (see this reference for the details of the simulations) in the so-called *calibration* case. It corresponds to MIMO 1×2 with *round robin* (RR) scheduler. We consider also other MIMO configurations and *proportional fair* (PF) scheduler, keeping all the other parameters unchanged. In particular, each base station always transmits its maximal power (*full buffer*).

According to [1], the 3GPP simulations consist in generating several realizations of the users positions, shadowing

MIMO	Scheduler	b	residual stand. dev.	b'
1×2	RR	0.83	0.45	0.98
1×2	PF	1.02	0.65	1.19
2×2	PF	0.67	0.74	1.08
4×2	PF	0.49	0.76	0.90

TABLE I
RESULTS OF THE LINEAR FITTINGS.

losses and fading channels. For each user location and each shadowing realization, the spectral efficiency is averaged over a large number of fading samples (about 1000). The value of the SINR including only the distance and the shadowing effects (and not fading) is also given. Then the spectral efficiency as function of the SINR is compared to the theoretical relation (10). More specifically, we make a linear regression between the spectral efficiency obtained from simulations and the theoretical efficiency given by Equation (10); that is we search for some b such that

$$s \simeq b \times S(\text{SINR}, t, r) \quad (11)$$

Table I gives the results of the linear fitting (11); i.e. the values of b and the corresponding residual standard deviation for different MIMO configurations³ (the first row corresponds to the calibration case [1, Table A.2.2-1]). Moreover, the 95%-confidence interval is about $b \pm 0.01$ for all the studied cases.

Figure 2 shows the spectral efficiency as function of the SINR from simulations and from the analytical expression (right-hand side of (11)) for the calibration case. Observe that the analytical expression reproduces well the general tendency of the empirical data obtained from simulations. The figures for the other cases listed in Table I are also generated, but not reproduced in the paper due to their similarity to Figure 2.

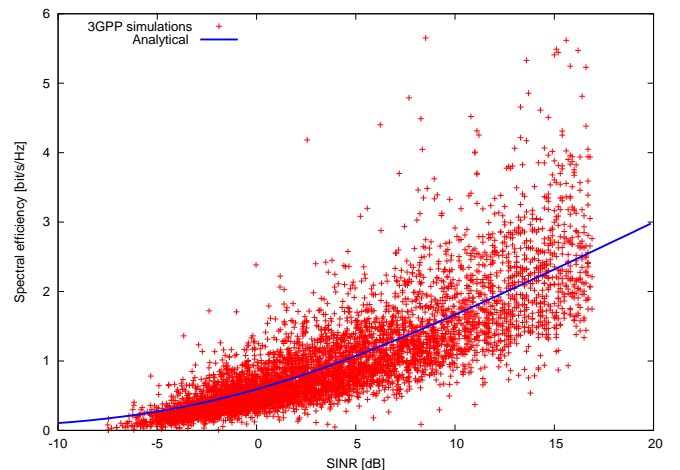


Fig. 2. Simulations versus the analytical expression (right-hand side of (11)) for the calibration case

Remark 3: In order to simplify the calculations we have also tested a linear regression between the spectral efficiency s obtained from simulations and the AWGN expression (9).

³All the considered cases have a MRC (Maximum Ratio Combining) receiver, except the MIMO 4×2 case which has a MMSE (Minimum Mean Square Error) receiver. At the base station side, the transmitting antennas are pairwise cross-polar. In the case MIMO 4×2 , the two cross-polar pairs of transmitting antennas are separated by 10 times the wavelength.

Observe from Equation (8) that when noise is dominant against interference, then

$$\text{SINR} = \frac{(P/t)/L_u}{N} = \frac{P/L_u}{N} \times \frac{1}{t}$$

Thus, in this particular case, the term $\frac{P/L_u}{N}$ in the right-hand side of (9) equals $\text{SINR} \times t$. Then, in the general case, it is natural to look for a fitting in the form

$$s \simeq b' \times a \log_2(1 + \text{SINR} \times t)$$

The resulting values of b' are indicated in Table I with residual standard deviations close to those indicated in the fourth column of that table.

C. SINR

For the analytical approach we use a similar geometric pattern of the network (hexagonal) and the same propagation-loss modeling regarding the distance and shadowing effects (fading has been already taken into account on the link level in the previous section) as the 3GPP calibration case [15, Table A.2.1.1-3] and [1, Table A.2.2-1].

More specifically, the frequency carrier is 2GHz. The distance loss model is $L = 128.1 + 37.6 \times \log_{10}(r)$ [in dB]. A supplementary penetration loss of 20dB is added. The shadowing is modeled as a centered log-normal random variable of standard deviation 8dB. The following 2D horizontal antenna pattern is used

$$A(\varphi) = -\min\left(12\left(\frac{\varphi}{\theta}\right)^2, A_m\right), \quad \theta = 70^\circ, A_m = 20\text{dB} \quad (12)$$

The system bandwidth is $W = 10\text{MHz}$, the noise power equals $N = -95\text{dBm}$ (-174dBm/Hz , noise figure=9dB) and the transmission power of the base station is $P = 60\text{dBm}$ (46dBm plus $G = 14\text{dBi}$ of antenna gain). The network is composed of 36 hexagons (6×6). Each hexagon comprises three sectors which gives a total of 108 sectors. The distance between the centers of two neighboring hexagons is 500m. We generate 3600 random user locations uniformly in the network; that is 100 user locations per hexagon in average.

The 3GPP simulations published in [1] are made on a planar network with random locations of the users. In the present study, two network models are considered: either planar or toroidal (to avoid the border effects).

Each mobile is served by the base station with the smallest *propagation-loss* (including distance, shadowing and antenna pattern). In order to facilitate the comparison of our results to those of 3GPP, we define the coupling-gain as the antenna gain G minus propagation-loss L with the serving base station. The cumulative distribution function (CDF)⁴ of the coupling-gain obtained by 3GPP simulations [1, Figures A.2.2-1 (left)] and by our models are given in Figure 3. This figure shows that the results of our planar network are close to those of 3GPP simulations, whereas those of toroidal network give larger coupling gain. This is due to the fact that in a planar network edge users get smaller coupling gain than in the toroidal one.

The SINR for each mobile is calculated by Equation (8), where u is the index of the serving base station. Figure 4 shows the CDF of the SINR coming from 3GPP simulations [1, Figure A.2.2-1 (right)] compared to that resulting from our

⁴over all the user locations in the network

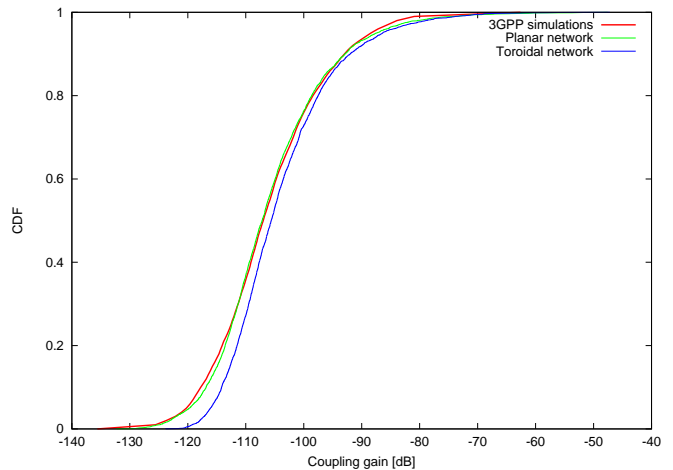


Fig. 3. CDF of the coupling gain (antenna gain minus propagation loss)

models. Again our planar model gives closer results to the 3GPP simulations than the toroidal one. Nevertheless, the difference between the SINRs of the toroidal and the planar networks is smaller than 0.5dB.

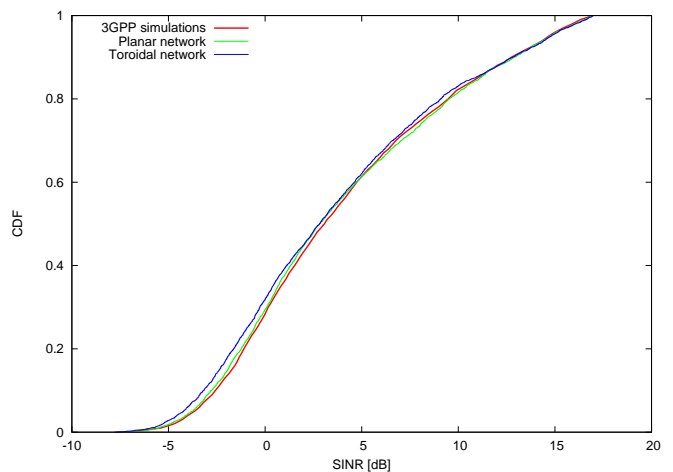


Fig. 4. CDF of SINR

Remark 4: Figure 4 shows that the SINR doesn't exceed 17dB. Indeed, each mobile served by a given base station (sector) is at least interfered by the two other sectors on the same site. The power received from each of these sectors is at least 10^{-2} times that received from the serving BS (this is related to $A_m = 20\text{dB}$ in Equation (12)). The interference to signal ratio is consequently larger than 2×10^{-2} i.e. -17dB which explains the observed upper limit of SINR.

Remark 5: Observe that the SINR defined by Equation (8) is different from the SINR calculated by 3GPP simulations which equals

$$\text{SINR}_{3\text{GPP}} = \frac{P/L_u}{N + P \sum_{v \neq u} 1/L_v}$$

However, if noise is negligible compared to interference, then the two SINRs are identical. This is the case in the considered urban scenario (small cell radius), so we have not to distinguish between these two SINRs.

MIMO	Scheduler	Arithmetic mean		Harmonic mean	
		Simus	Analytic	Simus	Analytic
1 × 2	RR	1.01	1.00	0.50	0.69
1 × 2	PF	1.32	1.23	0.80	0.85
2 × 2	PF	1.43	1.41	0.84	1.00
4 × 2	PF	1.54	1.54	0.95	1.18

TABLE II

CELL SPECTRAL EFFICIENCY: COMPARISON OF THE 3GPP SIMULATIONS AND THE ANALYTIC RESULTS.

D. Spectral efficiency

For each mobile we calculate the spectral efficiency corresponding to its SINR by relation (11). In order to facilitate the comparison of our results to those of 3GPP, we define the normalized user throughput as the spectral efficiency divided by 10 (this is historically related to the fact there are 10 users per cell in 3GPP simulations). The CDFs of the normalized user throughput obtained by 3GPP simulations [1, Figure A.2.2-3 (left)] and by our model are plotted in Figure 5. The 3GPP distribution is more spread than that of our models; this is related to the fact that the 3GPP spectral efficiency represents some variability around the analytic one as shown in Figure 2. Moreover, we observe that the results of the planar and toroidal models for the network are close to each other. Thus, the toroidal model is considered for the remaining part of the paper.

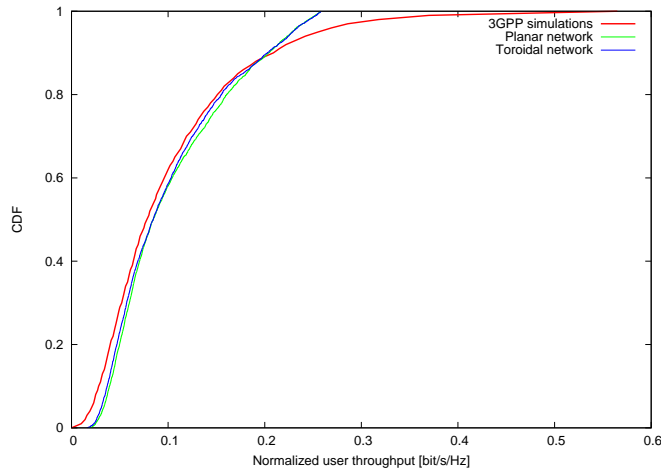


Fig. 5. CDF of normalized user throughput

Table II gives the *arithmetic mean* of the spectral efficiencies at the different locations (called cell spectral efficiency) for both 3GPP simulations and analytic approach. The results of two methods agree for all the considered MIMO and scheduler configurations.

Remark 6: Note that the results of the simulations given in Table II are produced by the simulator of Orange which is one of the contributors to 3GPP. The values indicated in [1, Table A.2.2-2] are in fact averaged over the different 3GPP contributors including Orange. In particular, for the calibration case (MIMO 1 × 2 with RR scheduler) Orange's result is 1.01 whereas 3GPP average is 1.1. The variability of the results among the contributors is partially due to the randomness induced by the shadowing.

IV. USER'S QoS CALCULATION

In order to illustrate the whole analytical approach, we show now how to calculate the QoS perceived by the users in a dynamic context; i.e., when users arrive and depart from the network. Variable bit-rate (VBR) calls such as mail, http, ftp are considered. Each VBR call aims to transmit some volume of data at a bit-rate which is decided by the network. Define the *peak bit-rate* at a given location as the bit-rate which may be allocated to some user in this location assuming that he is alone in the cell and that all the base stations transmit at their maximal powers. As observed by Caire and al. in [16, §I], for the VBR calls the performance at the link level for a given location should be firstly averaged over the fading; then these averages may be used at the queueing theory time scale to account for call arrivals and departures. Therefore we have a natural separation of the time scales of information theory and queueing theory. Assuming a round robin scheduler, the peak bit-rate at each location equals the system bandwidth times the spectral efficiency at that location given by Equation (11).

Let ρ be the traffic demand (in bit/s) per cell; that is the ratio of the average volume of data per call to the duration between two call arrivals to the cell. Assume that the traffic demand is uniformly distributed over the cell and that the users are allocated equal portions of the available resources (time and/or frequency). We assume that the users don't move during their calls.

In this context, queueing theory [17], [18, Example 10] shows that the user's throughput in the long run of the call arrivals and departures is given by

$$\bar{r} = \max(0, \rho_c - \rho) \quad (13)$$

where ρ_c is the so-called *critical traffic demand* which equals the *harmonic mean* of the peak bit-rates in the cell if the users don't move during their calls. On the opposite, if the users move during their calls, then the *critical traffic demand* equals the *arithmetic mean* of the peak bit-rates in the cell. At high mobility, the above formula holds also true with the appropriate critical traffic demand.

Consider the numerical setting of the calibration case described in Section III-C. Figure 6 shows the throughput per user in the cell as function of the cell radius for a traffic demand density 300kbit/s/km² (typical value in urban areas) for both the no-mobility and high mobility cases. We consider also the case when the interference is completely cancelled. As expected, the user's throughput decreases with the cell radius and ultimately vanishes for some critical cell radius. Moreover, observe that the mobility improves the user throughput from the queueing theory point of view as proved theoretically in [19, §VI]. On the other hand, observe that the interference cancellation improves performance, but this improvement decreases as the cell radius increases. For a cell radius of 0.3km, the interference cancellation increases the user throughput by a factor of about 7; whereas this factor is only of about 2 for cell radius of 2km. This is due to the fact that as the cell radius increases, the noise becomes dominant compared to interference.

The analytical approach developed in the present paper permits to make the parametric study represented in Figure 6

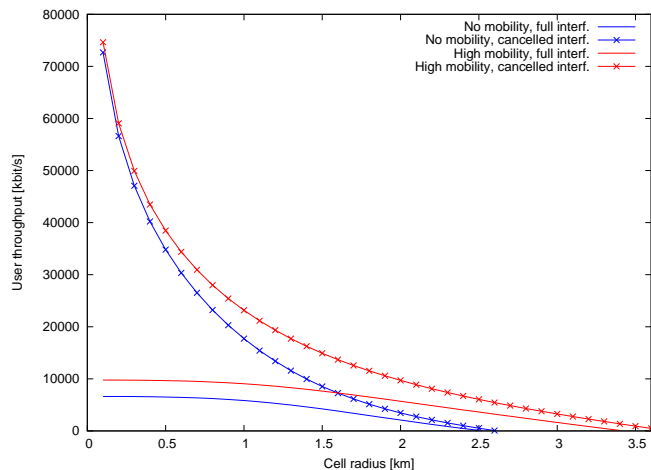


Fig. 6. User throughput as function of the cell radius in the cases of no mobility and high mobility (for the calibration scenario)

in about one minute; whereas it would require weeks for the 3GPP simulations.

Remark 7: Table II shows the harmonic means of the spectral efficiency obtained from 3GPP simulations and from the analytical expression. The difference may be explained as follows. Recall that the harmonic mean is sensitive to the minimal value of the considered data; for example if one of these data is null then the harmonic mean vanishes. Moreover, Figure 2 shows that the 3GPP spectral efficiency represents some variability around (and in particular comprise smaller values than) the analytic curve. This explains why the harmonic means obtained from simulations in Table II are lower than the analytic ones.

V. CONCLUSION

We describe a simple model of a MIMO cellular network which permits to obtain an analytical expression of users bit-rates which are feasible from the information theory point of view. This expression accounts for the variety of MIMO configurations (numbers of transmitting and receiving antennas) and radio conditions (SINR). This expression is compared to practical LTE performance evaluated by 3GPP simulations for different cases including the so-called calibration case. The comparison shows that the analytical expression may be adjusted to the practical performance by a multiplicative coefficient which depends on the MIMO configuration but not on the SINR. Additionally, we show the progress margin for potential evolution of the technology.

In order to illustrate the whole analytical approach, we calculate the throughput perceived by the users in the long run of users arrivals and departures in the network. The analytical approach permits to make the calculations in a much faster computing time than a purely simulation approach. The comparison of null and high user's mobility permits to quantify the effect of this mobility from the queueing theory point of view. Studying the case when interference is completely cancelled permits to quantify the ultimate improvement expected from the interference cancellation.

The simplifying assumption that the base stations are always transmitting (even when there are no users to serve) shall be

examined in the future work. Moreover, the QoS for other service classes such as streaming will be studied.

Acknowledgement: We thank B. Błaszczyszyn (INRIA), M. Debbah (Supelec) as well as A. Saadani, S. Jeux and A. Jassal (Orange Labs) for useful discussions related to the present paper.

REFERENCES

- [1] 3GPP, "TR 36.814-V900 Further advancements for E-UTRA - Physical Layer Aspects," in *3GPP Ftp Server*, 2010.
- [2] I. E. Telatar, "Capacity of multi-antenna Gaussian channels," *AT&T Technical Memorandum*, June 1995.
- [3] G. J. Foschini and M. J. Gans, "On limits of wireless communications in a fading environment when using multiple antennas," *Wireless Personal Communications*, vol. 6, no. 3, pp. 311–335, March 1998.
- [4] R. S. Blum, J. H. Winters, and N. R. Sollenberger, "On the capacity of cellular systems with MIMO," *Communications Letters, IEEE*, vol. 6, no. 6, pp. 242–244, jun 2002.
- [5] A. M. Tulino and S. Verdú, "Random matrix theory and wireless communications," *Foundations and Trends in Communications and Information Theory*, vol. 1, no. 1, 2004.
- [6] V. Tarokh, H. Jafarkhani, and A. R. Calderbank, "Space-time block coding for wireless communications: performance results," *IEEE J. Select. Areas Commun.*, vol. 17, no. 3, pp. 451–460, 1999.
- [7] S. M. Alamouti, "A simple transmit diversity technique for wireless communications," *IEEE J. Select. Areas Commun.*, vol. 16, no. 8, pp. 1451–1458, oct 1998.
- [8] S. Diggavi and T. Cover, "The worst additive noise under a covariance constraint," *IEEE Trans. Inf. Theory*, vol. 47, no. 7, pp. 3072–3081, 2001.
- [9] A. J. Goldsmith and S.-G. Chua, "Variable-rate variable-power MQAM for fading channels," *IEEE Trans. Commun.*, vol. 45, no. 10, pp. 1218–1230, 1997.
- [10] P. E. Mogensen, W. Na, I. Z. Kovács, F. Frederiksen, A. Pokhariyal, K. I. Pedersen, T. E. Kolding, K. Hugl, and M. Kuusela, "LTE Capacity Compared to the Shannon Bound," in *Proc. of VTC Spring, 2007*, pp. 1234–1238.
- [11] S. Ihara, *Information theory for continuous systems*. World Scientific, 1993.
- [12] 3GPP, "TR 36.942-V830 Evolved Universal Terrestrial Radio Access (E-UTRA) - Radio Frequency (RF) system scenarios," in *3GPP Ftp Server*, Sep. 2010.
- [13] —, "TR 36.211-V910 Evolved Universal Terrestrial Radio Access (E-UTRA) - Physical Channels and Modulation," in *3GPP Ftp Server*, Mar. 2010.
- [14] E. Dahlman, S. Parkvall, and J. Skold, *4g: LTE/LTE-advanced for mobile broadband*. Academic Press Inc, 2011.
- [15] 3GPP, "TR 25.814-V710 Physical layer aspects for evolved Universal Terrestrial Radio Access (UTRA)," in *3GPP Ftp Server*, 2006.
- [16] G. Caire, G. Taricco, and E. Biglieri, "Optimum power control over fading channels," *IEEE Trans. Inf. Theory*, vol. 45, no. 5, pp. 1468–1489, Jul. 1999.
- [17] J. W. Cohen, *On regenerative processes in queueing theory*, ser. Lecture Notes in Economics and Mathematical Systems. Springer Berlin Heidelberg, 1976, vol. 121.
- [18] M. K. Kararay, "User's mobility effect on the performance of wireless cellular networks serving elastic traffic," *Wireless Networks (Springer)*, vol. 17, no. 1, Jan. 2011.
- [19] T. Bonald, S. Borst, and A. Proutière, "How mobility impacts the flow-level performance of wireless data systems," in *Proc. of IEEE INFOCOM*, 2004, pp. 1872–1881.